Evaluation of the limit load capacity of masonry arch bridges

AMARYLLIS AUDENAERT
University College Antwerp, Artesis
Department of Applied Engineering
and Technology
Paardemarkt 92, 2000 Antwerpen
BELGIUM
amaryllis.audenaert@artesis.be
and
University of Antwerp
Department of Environment,Technology
and Technology Management
Prinsstraat 13, 2000 Antwerpen
BELGIUM

GENSERIK RENIERS
University of Antwerp
Department of Environment,Technology
and Technology Management
Prinsstraat 13, 2000 Antwerpen
BELGIUM
genserik.reniers@ua.ac.be

WOUT DULLAERT
University of Antwerp
Institute of Transport
and Maritime Management Antwerp
Prinsstraat 13, 2000 Antwerpen
BELGIUM
wout.dullaert@ua.ac.be

HERBERT PEREMANS
University of Antwerp
Department of Environment,Technology
and Technology Management
Prinsstraat 13, 2000 Antwerpen
BELGIUM
herbert.peremans@ua.ac.be

Abstract: Using a 2D decision support system based on a recent analytical model, this paper is the first to demonstrate that bridge specific characteristics require a detailed analysis to determine the collapse load. A parameterized study of the limit load capacity is necessary to calculate the worst case positioning of any kind of load. Because of the complexity of finite element modeling and the computation time requirements of 3D finite elements models for a large number of load positions, it is regularly assumed that collapse positions are situated at the crown of the arc. Empirical testing in this paper clearly demonstrates that this is not the case. The here developed approach allows for a quick scan of any type of masonry arch bridge, thus providing the necessary information on the critical range of load positions to be analyzed in more detail by a 3D modeling approach. Keywords

Key–Words: arches, collapse load, equilibrium,safety

1 Introduction

The analysis of load-bearing unreinforced masonry structures such as arches, vaults and buttresses has become the subject of renewed academic interest. The growing interest in the preservation of historical buildings and structures gives researchers the incentive, financially as well as socially, to develop methods of analysis for these structures. Moreover, arch bridges, which were designed in the days of horses and carriages are also required to function under the 21st century loadings. Nowadays, these structures are subject to heavy freight transport which they were originally not constructed for. The latter remark justifies the approach of studying the collapse behavior of these historical structures as accurately as possible. An extensive literature review on the topic is provided by Boothby [1].

The rigid block theory is the basic model for understanding the fundamental behavior of masonry arches [2, 3, 4]. This theory simplifies the masonry arch structure as a collection of rigid blocks and calculates its stability using the principle of virtual work,which is an alternative way of expressing the equations of motion and equilibrium. This principle is often used in mechanics of structures and is also the basis of FEM-models [5]. Eventually the rigid-block methodology gives rise to an upper bound for the collapse load for a given load position and thus offers a first quick insight into the arch behavior. The collapse load is an objective measure to determine the bearing capacity of a structure.

A more recent research technique uses finite element analysis. The models range from 1-dimensional [6, 7], over 2-dimensional [8, 9], up to fully 3-dimensional models [10, 11] for understanding three-dimensional effects. These 3D-models do require a precise knowledge of parameters which are usually not well-known in practice. Moreover, finite element programs are often computationally expensive and require a high level of modelling expertise.

A major shortcoming of both the rudimental rigid block method and the more accurate 3-dimensional finite element analysis is their inability to carry out detailed sensitivity analysis. Software based on these models can only assess an arch bridge for specific load conditions and parameter settings. Neither the influence of material properties, nor the influence of different loadings can be evaluated easily. Especially for determining the bearing load on arch bridges, such a parameter analysis might prove to be very important.

To alleviate these modelling shortcomings, this paper embeds an analytical model for determining the collapse load for a single loading position in a decision support tool. The resulting software is capable of identifying the specific position (of the load) which allows the smallest collapse load, thus governing the safety of the arch.

To determine the bearing capacity of an arch bridge, we first determine the collapse load for all possible load positions on the bridge using an analytical model.

2 Equilibrium equations

The starting point for this analysis is the derivation of the three equilibrium equations, i.e. horizontal, vertical and moment equilibrium that must be satisfied in every point of an arch bridge. They are written down as continuous equations, as opposed to the discrete approach taken in a finite element analysis. The geometry of the arch is determined by the angle θ, the radius $r(\theta)$ and the thickness $b(\theta)$ as shown in Fig 1.

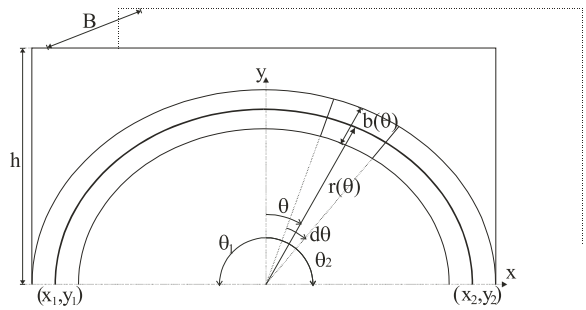

Figure 1: Definition of the geometrical parameters of an arch in function of θ

All these geometrical parameters are function of the angle θ, capable of modelling any shape of arch barrel.

2.1 Equilibrium of an infinitesimal element of arch

To derive the differential equilibrium equations the equilibrium of an infinitesimal piece with unit width, angular extent $d\theta$, of the arch is considered, as in Fig 2.

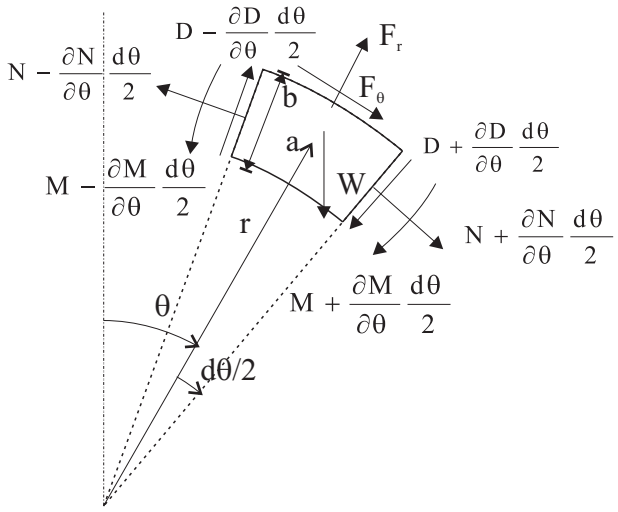

Figure 2: Equilibrium of an infinitesimal slice of arch

From Fig 2 the equilibrium of an infinitesimal slice of arch implies the balance of the internal forces and moments, i.e. the normal force N (> 0 for tension), the shear force D (> 0 for a clockwise rotation) and the bending moment M (> 0 for compression in the intrados), the weight of this segment of arch and the external forces applied to it. The external forces applied to the arch act on the extrados. As shown in Fig 2, they are the forces F_r , acting in the radial direction, and F_θ , acting in the tangential direction. Hence, the three equilibrium equations are :

$$-W(\theta)cos(\theta) - Nd\theta - \frac{\partial D}{\partial \theta}d\theta + \sum F_r = 0 \quad (1)$$

$$W(\theta)sin(\theta) - Dd\theta + \frac{\partial N}{\partial \theta}d\theta + \sum F_\theta = 0 \quad (2)$$

$$\frac{\partial M}{\partial \theta}d\theta + N\frac{\partial r}{\partial \theta}d\theta + Drd\theta + M_a(W) + M_a(F) = 0 \quad (3)$$

with $M_a(W)$ and $M_a(F)$ denoting the moments of the weight and the external forces with respect to

the point a (Fig 2). Below, expressions will be derived for the terms involving the weight and the external forces.

2.2 Weight of an infinitesimal slice of arch

In this section, the weight and the center of gravity of this infinitesimal slice of arch are determined. As shown in Fig 2 the total weight is given by the weight of the large triangular segment of arch (base = r+b/2) minus the weight of the small triangular segment of arch (base = r-b/2), neglecting second order terms.

$$W(\theta) = \frac{1}{2}\gamma[(r+\frac{b}{2})^2 - (r-\frac{b}{2})^2] = \gamma b r d\theta \quad (4)$$

$$r_G(\theta) = r(1+\frac{b^2}{12r^2}) = r(1+\frac{\eta^2}{12}) \quad (5)$$

with γ the specific weight [N/m3] of the material, r_G the radius of the centerline, B the width of the arch, b the height of the arch barrel and $\eta(\theta) = \frac{b(\theta)}{r(\theta)}$. As the center of gravity does not coincide, in general, with the point a there will be a moment associated with this weight.

$$M_a(\theta) = \gamma r^3 \frac{\eta^3}{12} sin\theta d\theta \quad (6)$$

2.3 External loads acting on an infinitesimal slice of arch

To take into account the external loads acting on an infinitesimal slice of arch a distinction is drawn between distributed loads and concentrated loads.

2.3.1 Distributed loads

For each infinitesimal slice of arch the distributed loads acting on it are summarized by a radial force p_r and a tangential force p_θ. As an example, the distributed load is derived for an infinitesimal piece of the arch resulting from the infill carried by that slice of arch.

The total vertical load, neglecting second order terms, caused by the infill carried by the slice of the arch shown in Fig 3 is given by

$$V(\theta) = \gamma_2[h-(r(\theta)+\frac{b(\theta)}{2})cos\theta](r(\theta)+\frac{b(\theta)}{2})cos\theta d\theta \quad (7)$$

with γ_2 denoting the specific weight [N/m3] of the homogeneous material used for the infill and h the height

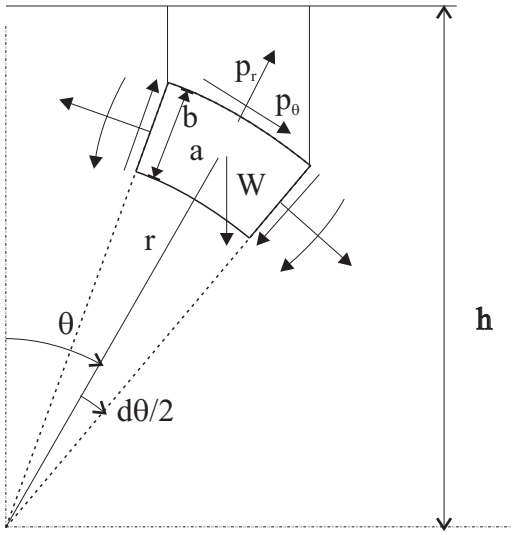

Figure 3: Distributed load resulting from infill carried by arch

of the arch plus the superstructure. Splitting this load in a radial and a tangential component yields

$$\begin{aligned}\sum F_r &= -V(\theta)cos\theta \\ &= -\gamma_2[h-(r(\theta)+\frac{b(\theta)}{2})cos\theta] \\ &\quad (r(\theta)+\frac{b(\theta)}{2})cos^2\theta d\theta \\ &= p_r d\theta \end{aligned} \quad (8)$$

$$\begin{aligned}\sum F_\theta &= -V(\theta)sin\theta \\ &= -\gamma_2[h-(r(\theta)+\frac{b(\theta)}{2})cos\theta] \\ &\quad (r(\theta)+\frac{b(\theta)}{2})cos\theta sin\theta d\theta \\ &= p_\theta d\theta \end{aligned} \quad (9)$$

$$\sum M_a(F) = p_\theta \frac{b}{2} d\theta \quad (10)$$

Next, a load is examined that is no longer distributed over the surface of the arch but acts in a single, isolated, point as shown in Fig 4.

2.3.2 Concentrated load

A Dirac distribution is defined by

$$\delta(\theta-\alpha) = 0, \quad \theta \neq \alpha \quad (11)$$

$$\int_{-\infty}^{+\infty} \delta(\theta-\alpha)d\theta = 1 \quad (12)$$

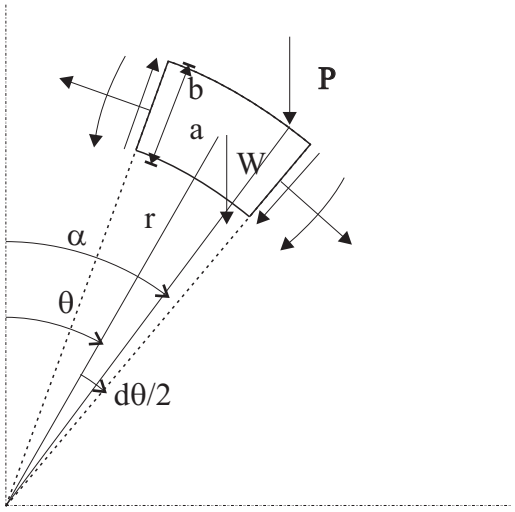

Figure 4: Concentrated load

as a mathematical model for the concentrated load. As can be seen from this definition the Dirac distribution is zero everywhere except at $\theta = \alpha$ where its value is defined implicitly by the integral expression. This formulation will allow the integration of both distributed and concentrated loads in a single mathematical framework. A concentrated load of intensity P that applies at $\theta = \alpha$ (see Fig 4) will then be denoted by $P\delta(\theta - \alpha)$.

In this case, the contributions from a concentrated vertical load to the three equilibrium equations become respectively :

$$\sum F_r = -P\delta(\theta - \alpha)cos\theta d\theta \tag{13}$$

$$\sum F_\theta = P\delta(\theta - \alpha)sin\theta d\theta \tag{14}$$

$$\sum M_a(F) = P\delta(\theta - \alpha)|r(\alpha)sin\alpha - r(\theta)sin\theta|d\theta \tag{15}$$

3 Solving the equilibrium equations

Audenaert et al. [12] show how the equilibrium equations can be transformed to a set of ordinary differential equations (16), (17) and (18) to calculate normal forces $N(\theta)$, shear forces $V(\theta)$ and bending moments $M(\theta)$.

$$-V' - N - \gamma r^2 \eta cos\theta + p_r - \sum_i P_i\delta(\theta - \alpha_i)cos\theta + \sum_j H_j\delta(\theta - \alpha_j)sin\theta = 0 \tag{16}$$

$$N' - V + \gamma r^2 \eta sin\theta + p_\theta + \sum_i P_i\delta(\theta - \alpha_i)sin\theta + \sum_j H\delta(\theta - \alpha_j)cos\theta = 0 \tag{17}$$

$$M' + Nr' + Vr + \gamma r^3 \frac{\eta^3}{12}sin\theta + p_\theta \frac{b}{2} + \sum_i P_i\delta(\theta - \alpha_i)|r(\alpha_i)sin\alpha_i - r(\theta)sin\theta| + \sum_j H_j\delta(\theta - \alpha_j)|r(\alpha_j)cos\alpha_j - r(\theta)cos\theta| = 0 \tag{18}$$

In equations (16), (17) and (18) a prime denotes the derivative with respect to θ; p_r = the radial distributed force; p_θ = the tangential distributed force; α_i = the position of the vertical point load P_i; α_j = the position of the horizontal point load H_j; γ = the specific weight of the arch and $\eta = \frac{b}{r}$.

The general solution of the set of differential equations derived above includes three constants, i.e. k_1, k_2 and k_3. Hence, to find the unique solution for the internal forces and the bending moment in the arch bridge we require additional constraints. The boundary conditions introduced below are constraints on the horizontal, vertical and angular deflections of the fixation points of the arch bridge.

The so-called Bresse equations [13], yield expressions for these deflections, based on the following assumptions:

- symmetric cross section
- load applied in the symmetry plane (deformed centerline remains in the symmetry plane)
- linear elastic material

Note that the second condition is trivially satisfied as we consider a 2D model and the third condition describes the material behavior in between the hinges. As the arch bridges and external load conditions studied here satisfy the first and the last condition the equations of Bresse express the deflections in every point of the arch bridge, in terms of the values for these deflections in one of the boundary points. In particular, Bresse's equations yield the deflections in the right fixed support, given their values in the left

fixed support :

$$\varphi_2 = \varphi_1 + \frac{1}{E}\int_{\theta_1}^{\theta_2} \frac{M}{I}\sqrt{r^2 + (\frac{\partial r}{\partial \theta})^2}d\theta \quad (19)$$

$$u_2 = u_1 + (y_2 - y_1)\varphi_1 + \frac{1}{E}\int_{\theta_1}^{\theta_2} \frac{N}{A}\frac{\partial x}{\partial \theta}d\theta + \frac{1}{E}\int_{\theta_1}^{\theta_2} (y_2 - y)\frac{M}{I}\sqrt{r^2 + (\frac{\partial r}{\partial \theta})^2}d\theta \quad (20)$$

$$v_2 = v_1 - (x_2 - x_1)\varphi_1 + \frac{1}{E}\int_{\theta_1}^{\theta_2} \frac{N}{A}\frac{\partial y}{\partial \theta}d\theta - \frac{1}{E}\int_{\theta_1}^{\theta_2} (x_2 - x)\frac{M}{I}\sqrt{r^2 + (\frac{\partial r}{\partial \theta})^2}d\theta \quad (21)$$

with

$\varphi =$ rotation of the elastic line

$u =$ horizontal deflection

$v =$ vertical deflection

$A =$ area of the cross-section

$I =$ rotational inertia of the cross-section

$E =$ modulus of elasticity

$x =$ horizontal position coordinate

$y =$ vertical position coordinate

and the subscripts 1 and 2 denoting the left and the right support of the arch bridge respectively, see Fig 1. The sign conventions for the horizontal and vertical deflections u and v are taken to be the same as for the x-axis and y-axis, the rotation φ is taken to be positive for clockwise rotations. Both axes are defined as shown in Fig 1. If the deflections in both supports, i.e. (u_1, v_1, φ_1) and (u_2, v_2, φ_2), are specified these equations can be used to derive unique values for k_1, k_2 and k_3. This can be understood by noting that all three functions $N(\theta)$, $V(\theta)$ and $M(\theta)$, as derived above, are linear functions of the unknown constants k_1, k_2 and k_3. Furthermore, all operators applied to $N(\theta)$ and $M(\theta)$ in Bresse's equations are linear as well. Hence, inserting the expressions derived for $N(\theta)$ and $M(\theta)$, in Bresse's equations will yield a linear set of equations in terms of the unknown constants k_1, k_2 and k_3. By putting all known terms on the left side of the equations, i.e. E_i and the terms containing k_i on the right side, this can be rewritten using matrix notation as :

$$\overline{E} = A\overline{k} \quad (22)$$

with $\overline{E} = [E_1\ E_2\ E_3]^\tau$, $A = [a_{ij}]$ and $\overline{k} = [k_1\ k_2\ k_3]^\tau$.

Whenever matrix A is non-singular this matrix equation can be solved to find the unique set of constants k_1, k_2 and k_3. Therefore, this method allows to find the unique solution of the equilibrium equations for a linear elastic arch.

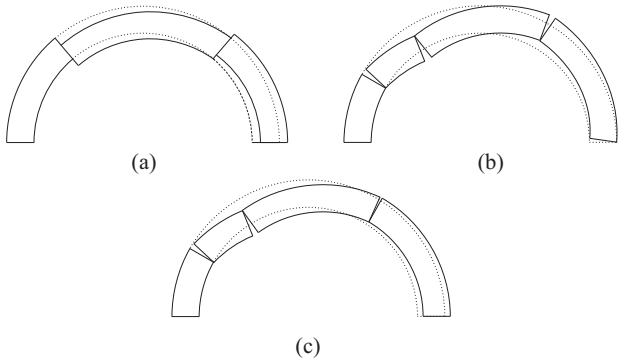

Figure 5: Collapse modes

The sign conventions for the horizontal and vertical deflections u and v are taken to be the same as for the x-axis and y-axis, the rotation φ is taken to be positive for clockwise rotations. Both axes are defined in Fig. 1. If the deflections at both supports are specified, these equations can be used to calculate the internal forces $N(\theta)$, $V(\theta)$ and $M(\theta)$.

To calculate the stability of an arch, a failure criterium is added to the model.

According to [2], an arch bridge can collapse as a result of three possible collapse mechanisms : a shear mechanism (Fig 5(a)), a hinge-mechanism (Fig 5(b)) and a combined shear-hinge mechanism (Fig 5(c)).

Figure 6: Collapse of the Bridgemill arch bridge. (Source: http: //archive. niees.ac.uk/talks/dem/nenad_bicanic.ppt)

Experiments by Hendry et al. [14] and by others show that, due to most arches being well-buttressed,

the hinge-mechanism (Fig.6) can be considered as by far the most likely collapse mechanism for arches. Therefore this paper focusses on this mechanism.

The formation of hinges and the complementary propagation of cracks needs we assume that the first crack will appear at the position for which a defined tensile strength σ_t is reached. When the compressive strength σ_d is reached, the material behaves perfectly plastic finally resulting in a hinge. How these material properties are included into the analytical model is thoroughly explained in [15]. The solution of the differential equations can be found in [12].

Initially, the arch does not contain any hinges. The smallest value of the load that gives rise, to a relative normal force and a relative moment that satisfy equation (25) is the value P_{max1} corresponding with the first hinge. The angle $\theta = \theta_{max1}$ corresponding with this value P_{max1} gives the location of this first hinge.

In the presence of one plastic hinge the arch turns into a structure statically indeterminate to the second degree. Afterwards, an arbitrary rotation can occur in this hinge with a constant bending moment, while the material can be considered elastic in other cross sections. The equations of equilibrium remain the same for an increasing load, but the boundary conditions are adjusted to represent the changed conditions.

This procedure will be repeated until the arch turns into an four hinge mechanism. At that moment the collapse load is known as well as the position of the 4 hinges.

3.1 Elastic-plastic material properties

It is clear that to get good correspondence between theory and experiment we will have to extend the model presented here to take into account the material properties. In particular, since arch bridges are mostly concrete, masonry or stone constructions, the presence of cracks will have to be taken into account.

Masonry is a very complex composed material. As shown by Cecchi [16], [17]and Milani [**?**], homogenization procedures exist to allow assessment of masonry as an homogenous material.

The following assumptions are made with respect to the behavior of the material:

- on reaching the tensile strength σ_t a crack occurs;
- on reaching the compressive strength σ_d the material behaves perfectly plastic;
- for $\sigma_d < \sigma < \sigma_t$ the material behaves linearly elastically.

The tensile strength of masonry is accepted to have little influence and to be negligible compared to the compressive strength [**?**], hence we set $\sigma_t = 0$. In the examples shown below we choose a typical value for the compressive strength, i.e. $\sigma_d = -8Mpa$.

Only a limited number of stress distributions can occur under these assumptions : a linear-elastic distribution, an elasto-fragile distribution, an elasto-plastic distribution, an elasto-plasto-fragile distribution and a plasto-fragile distribution.

Fig 7 shows the evolution of the stress distribution when a cross-section of the arch bridge is subjected to an increasing pressure load, with

$x_f =$ height of the crack,

$x_p =$ height of the plastic section

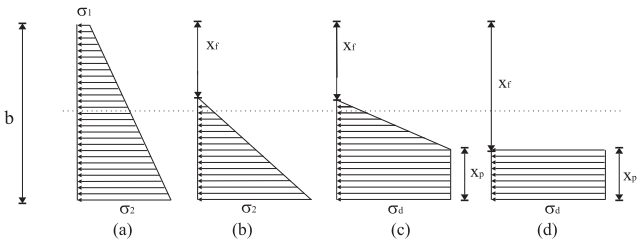

Figure 7: Evolution of the distribution of stress as the pressure load is increased from (a) to (d).

Next, we introduce normalized versions of $N(\theta)$ and $M(\theta)$, i.e. the relative normal force $n_d(\theta)$ and the relative moment $m_d(\theta)$.

$$n_d(\theta) = \frac{N(\theta)}{-\sigma_d b(\theta)} \quad (23)$$

$$m_d(\theta) = \frac{M(\theta)}{-\sigma_d b^2(\theta)} \quad (24)$$

Each of the possible stress distributions will mark out a zone in the (n_d, m_d) -plane, which contains combinations of the relative normal force $(= n_d)$ and the relative moment $(= m_d)$ in which that specific distribution is possible, as shown in Fig 8.

The border of the elasto-plasto-fragile area corresponds to a plasto-fragile distribution, corresponding to the stress distribution shown in Fig 7(d), and reflects those combinations that correspond to the stress distribution of a plastic hinge.

The equation that describes this envelope in the compression region is obtained by eliminating x_f and x_p from the expressions for n_d and m_d that apply to the situation shown in Fig 7(d) :

$$|m_d| = \frac{-n_d^2 - n_d}{2} \quad (25)$$

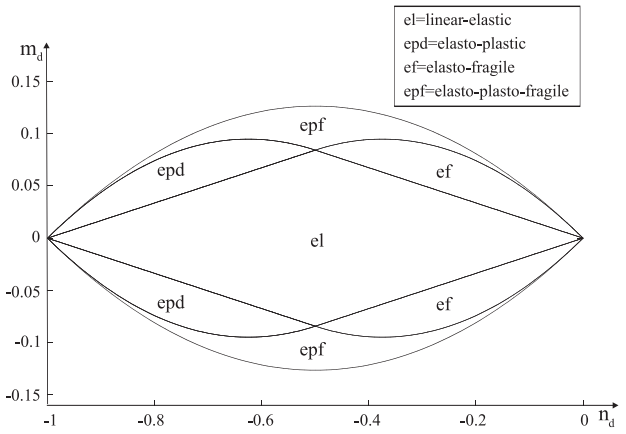

Figure 8: Envelope of the distribution of stress

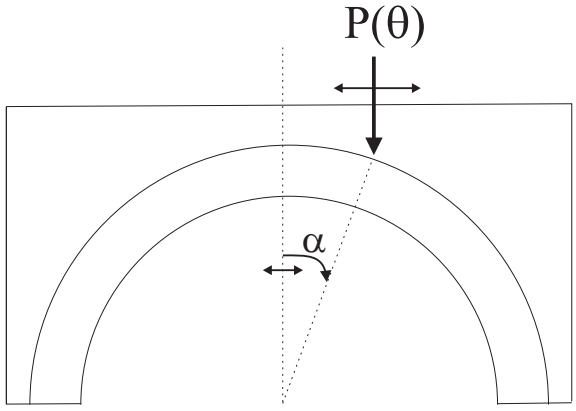

Figure 9: Algorithm to determine the bearing cappacity of the arch in function of the load position.

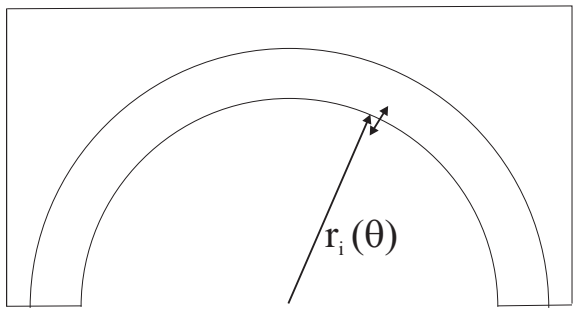

Figure 10: Algorithm to determine the variation in critical load position in function of the arch geometry.

4 2D decision support system

Current research predicts arch bridge behavior under a given load. However, such studies do not offer information about the bearing capacity of an arch bridge. The analytical model from Section 2 allows for an efficient sensitivity analysis on loading positions to determine the corresponding collapse load. The minimum of these collapse loads determines the ultimate allowable load for a given bridge geometry. In this section we will examine whether the critical load position differs for bridges with different geometry.

Bridges have primarily been built to resist vertical loads. Thus, in the case of a vertical concentrated load, the safety assessment of the bridge should be performed for all possible load positions α. The position giving rise to the smallest value for the collapse load determines the bearing capacity of the arch. Figure 9 visualizes this bearing capacity procedure. Hence, we perform a search of the load position and compute the collapse load. The advantage of this approach is that it quickly gives the ultimate overview of the arch bridge's behavior.

To illustrate the necessity and workings of the quick scan methodology, consider the following set of semi circular masonry arch bridge features. All bridges are assumed to have the same material properties, infill, and radius of the outer curve of the arch (extrados r_e) (see Figure 10).

The bridges with unit width only differ in their radius of the inner curve of the arch, the so-called intrados r_i. The height of the infill h is 2 meters and the specific weight of the infill γ_2 is 21600 N/m^3 corresponding to a traditional sandbased infill. The masonry barrel is assumed to have a specific weight of 21000 N/m^3, an elasticity coefficient of 5 GPa, compressive strength of -8 MPa and tensile strength of zero reflecting the masonry's inability to resist tensile. The radius of the intrados r_i varies between 1.4 and 1.7 meters implying a variation in barrel thickness in the range of [0.5-0.2] given the fixed radius of the extrados $r_e = 1.9m$. The position of the point load P varies from $-1 = -57.30°$ to $1 = 57.30°$.

In Fig.11 the collapse load is shown in function of all position of the load, α, and in function of the radius of the intrados, r_i. The results support common wisdom that ticker arch barrels can resist higher collapse loads.

$r_i[m]$	$P_{collapse}[kN]$	$\alpha[rad]$	$\alpha[°]$
1.4	56.51	0.25	14.32
1.5	30.80	0.2	11.46
1.6	14.94	0.15	8.59
1.7	5.22	0.1	5.73

Table 1: Collapse loads and most dangerous load positions for different arch geometries

In Table 1 the numerical results for the load position giving rise to the smallest collapse load end the corresponding collapse load are listed for some arch

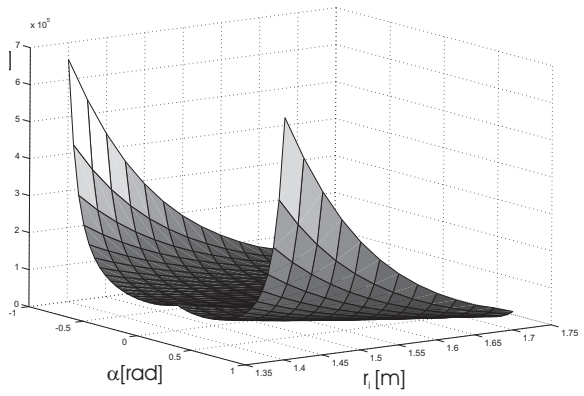

Figure 11: Collapse load in function of α and r_i

geometries.

Also the higher the barrel of the arch, the more the weakest point of the arch (i.e., the location α corresponding with the smallest collapse load) differs from the crown of the arch.

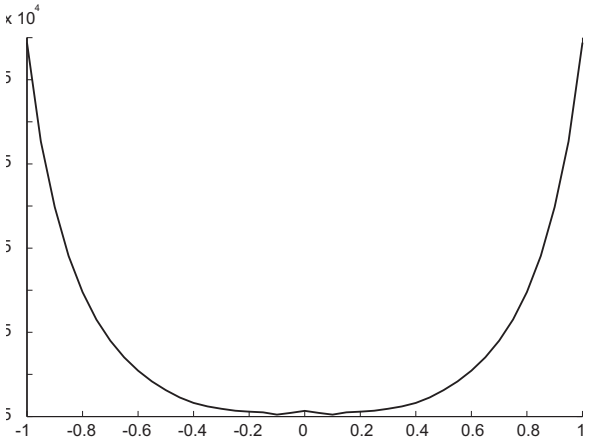

Figure 12: Collapse load in function of α for the smallest arch, $r_i = 1.7$

For the biggest and the smallest arch the collapse load in function of the load position are shown respectively in Fig.12 and Fig.13.

In Table 2 the overall collapse load is compared to the the collapse load corresponding to the crown of the arch ($\alpha = 0$).

$P[kN]$		$\alpha[rad]$					$\% - \varepsilon$
		0	0.1	0.15	0.2	0.25	
$r_i[m]$	1.4	73.44				56.51	29.96
	1.5	35.38			30.80		14.87
	1.6	16.08		14.94			7.63
	1.7	5.67	5.22				8.62

Table 2: Influence of α on the collapse load for different arch geometries.

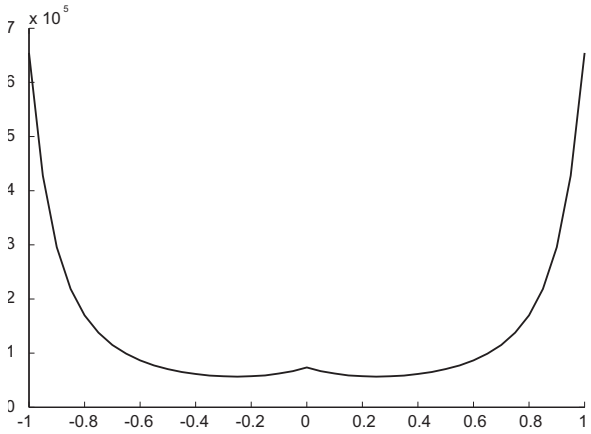

Figure 13: Collapse load in function of α for the thickest arch, $r_i = 1.4$

For each arch geometry only these two values are listed in the table. Also the corresponding $\%$-error is calculated. Especially for a thick arch geometry $(r_i = 1.4)$ the overall collapse load for a load positioned at $\alpha = 0.25$ differs significantly, approximately 30%, from the collapse load obtained for $\alpha = 0$. For smaller arch barrels the error-percentage diminishes, but remains larger than 8%. These results indicate that for every bridge one should conduct a sensitivity analysis based on an investigation of the weakest position of the arch.

The latter findings are in accordance with the findings of Brencich et al. [19] demonstrating that $\alpha = 0$ is not the weakest point of the bridge. As Brencich used a FEM-program for this calculations he was only able to evaluate a limited number of load positions. The computation time requirements of his FEM approach therefore excludes an extensive sensitivity analysis required for assessing the safety of arch bridges. Our method is capable of doing a fast and very accurate parameter analysis in function of the load position.

5 Conclusions

Determining a "safe load carrying capacity" of arch bridges continues to challenge civil servants and researchers. The proposed method of strength assessment described in this paper advances the state-of-the-art in two-dimensional modeling of masonry arch bridges. Our two-dimensional assessment algorithm serves as a conservative, computationally efficient approach to tackle safety of such masonry arch bridges.

Previous models from the literature assess arches under a given specific load condition. Because of the complexity of finite element modeling and the compu-

tation time requirements of 3D finite elements models for a large number of load positions, it is regularly assumed that collapse positions are situated at the crown of the arc.

An analytical approach to the collapse analysis of single-span arch bridges is presented above. This procedure makes possible a fast and reasonably accurate determination of the assessment of an arch under a wide range of load-conditions. Both the locations of the hinges and the collapse load of an arch bridge can be determined. The analytic approach makes it possible to perform parameter studies, e.g. determine the weakest point of an arch bridge

Our methodology investigates the safety of arches under different conditions using sensitivity analysis.Computational testing shows that the weakest point of an arch is different for every geometry, which means that no assumptions about this matter can be made beforehand. The critical position differs from the crown of the arch and should therefore be determined for every single arch geometry. A small variation in geometry or material properties is shown to have a significant influence on the bearing capacity of the arch.

To obtain an even better match between the theoretical results and the behavior of the real bridge more detailed modeling of the bridge is required, e.g. taking into account sliding phenomena as well as the presence of infill and spandrel walls. Also, being a 2-dimensional model, it cannot fully take into account the non-zero width of the bridge.

The approach developed in this paper allows for a quick scan of any type of masonry bridge, thus providing the necessary information on the critical range of load positions to be analyzed in more detail by a 3D modeling approach [20].

References:

[1] T. Boothby, Analysis of masonry arches and vaults, *Progress in Structural Engineering and materials*, 3,2001,pp. 246-256

[2] T. Boothby, Collapse modes of masonry arch bridges, *Journal of the british masonry society*, 9(2),1995,pp.62-69

[3] M. Gilbert and C. Melbourne, Rigid-block analysis to masonry arches,*Structural Engineering*, 72,1994,pp. 356-361

[4] T.G. Hughes and M.J. Blackler, A review of the UK masonry assessment methods, *Proceedings of the Institution of Civil Engineers*, 110, 1995,pp.373-382

[5] W. Wunderlich, Mechanics of Structures: Variational and Computational Methods, CRC, ISBN0849307007, 2002

[6] B.S. Choo, M.G. Coutie and N.G. Gong, Finite-element analysis of masonry arch bridges using tapered elements, *Proceedings of the Institution of Civil Engineers*, 91,1991,pp. 755-770

[7] C. Mollins and P. Roca,P.,Capacity of masonry arches and spatial frames, *Journal of structural engineering*, 124,1998,pp. 653-663

[8] T.E. Boothby, D.E. Domalik and V.A. Dalal, Service load response of masonry arch bridges, *Journal of structural engineering*, 124,1998,pp. 17-23

[9] K.H. Ng, C.A. Fairfield and A. Sibbad, Finite-element analysis of masonry arch bridges, *Proceedings of the Institution of Civil Engineers : Structures and Buildings*, 134, 1999, pp.119-127

[10] P.J. Fanning, T.E. Boothby and B.J. Roberts, Longitudinal and transverse effects in masonry arch assessment, *Construction and Building Materials*, 15,2001, pp. 51-60

[11] P.J. Fanning, L. Sobczak, T.E. Boothby, T.E. and V. Salomoni, Load Testing and Model Simulations for a Stone Arch Bridge, *Bridge Structures* , 1(4),ISSN 1573-2487, 2005

[12] A. Audenaert,H. Peremans and G. Reniers,2007,An analytical model to determine the ultimate load on masonry bridges, *Journal of Engineering Mathematics*, 59:3,2007, pp. 323-336

[13] M. Bresse, *Cours de Mécanique Appliquée*, Imprimerie de Gauthier-Villars (Paris),, 1859

[14] A.W. Hendry, S.R. Davies and R. Royles, Test on a Stone Masonry Arch at Bridgemill-Girvan. *Transport and Road REsearch Lab, Contractors Report 7 United Kingdom*,1985

[15] A. Audenaert,A., H. Peremans and W.P. De Wilde,Static determination of the internal forces and displacements in arch bridges, *The Masonry Society Journal*, 22(1),2004, pp.97-109

[16] A. Cecchi, CFRP reinforced masonry walls: analytical and numerical homogenised models, *WSEAS Transactions on Applied and Theoretical Mechanics*, Vol.1, No.1, 2006, pp. 7-15.

[17] A. Cecchi, A. Barbieri, Homogenisation procedure to evaluate the effectiveness of masonry strengthening by CFRP repointing technique

WSEAS Transactions on Applied and Theoretical Mechanics,

Issue 1, Volume 3, January 2008 12-27

[18] G. Milani, A simple equilibrated homogenization model for the limit analysis of masonry structures. *WSEAS Transactions on Applied and Theoretical Mechanics*, Vol.2, No.5, 2007, pp. 119-125.

[19] A. Brencich,U. De Francesco, and L. Gambarotta,Elastic no tensile resistant-plastic analysis of masonry arch bridges as an extension of Castigliano's method, *9th Canadian masonry symposium*, Frederiction(Canada),2001

[20] A. Audenaert, P. Fanning,L. Sobczak and H. Peremans,2D analysis of masonry arch bridges using an elasto-plastic material model, *Engineering structures: the journal of earthquake, wind and ocean engineering* , 30:3(2008), 2008,pp. 845-855